ELSEVIER

Comput. Methods Appl. Mech. Engrg. 148 (1997) 209–224

Computer methods in applied mechanics and engineering

Implicit time splitting for fourth-order parabolic equations

C.I. Christov [a,*,1], J. Pontes [b,c], D. Walgraef [b], M.G. Velarde [a]

[a] *Instituto Pluridisciplinar, Universidad Complutense, Paseo Juan XXIII, Madrid 28040, Spain*

[b] *Service de Chimie-Physique, Université Libre de Bruxelles Campus Plaine – CP231, Bruxelles 1050, Belgium*

[c] *Promon Engenharia ltda. Praia do Flamengo 154 22210 Rio de Janeiro RJ, Brazil*

Received 12 July 1993; revised 11 January 1996; accepted 26 August 1996

Abstract

A coordinate-splitting economic difference scheme is proposed for generalized parabolic equations (GPE) containing fourth-order diffusion operators and the algorithm for its implementation is developed. The performance of the scheme is demonstrated for different cases, e.g. for treating bifurcation phenomena. The technique is applied to the numerical solution of Swift–Hohenberg equation describing the Rayleigh–Bénard convection and results are obtained for very large system sizes and for very long times on small computational platform.

1. Introduction

The description of physico-chemical systems close to pattern forming instabilities leads to dynamical models based on nonlinear PDE with higher-order spatial derivatives that may be called Generalized Diffusion Equations. The lowest-order nontrivial generalization of the diffusion equation involves fourth-order spatial derivatives. Save for the limited number of cases when analytic solutions are available, the only way to obtain information from the models is by means of numerical solution.

Creating effective numerical schemes and algorithms for diffusion equations and their generalizations enjoy considerable attention due to important applications of these models. A variety of different schemes has been created for the equation with second-order diffusion (heat-conduction equation). The time stepping of the solution can be done either by spectral (see the illuminating work [5]) or by explicit or implicit schemes with finite differences or finite elements, or by certain combination of these. In [4] an explicit scheme allowing vectorization is proposed for the advection–diffusion equation. The condition of stability of an explicit scheme imposes, as a rule, very restrictive limitations on the time increment. It is much more true for the fourth-order derivatives when $\tau \leqslant 1/4h^4$. That is why the problem of constructing implicit schemes is of significance. However, the straightforward implementation of an implicit scheme in more than one spatial dimension results in very large linear systems whose solution is tenable only on super-computers, which rule out their use on smaller computer platforms.

An effective way to combine the stability properties of implicit schemes and the cost-efficiency of the explicit ones is to use the so-called coordinate splitting. The time step is implemented through several *half-time steps* in which only one of the operators is implemented implicitly. The notion of splitting was

*Corresponding author.

[1] Present address: National Institute of Meteorology and Hydrology, Bulgarian Academy of Sciences, 66 Tsarigradsko Chaussee blvd., Sofia 1784, Bulgaria

PII S0045-7825(96)01176-0

introduced in [13,3] for the second-order parabolic equation (heat equation) and proved very fruitful (see [19] for review of the earlier results).

The coordinate splitting method is still one of the most popular techniques for solving advection–diffusion problems. In [10] is developed an Alternating Directions Implicit (ADI) scheme for studying solidification problems where special care is needed since the temperature oscillations in the interface between the phases may cause instability. In [8] is applied so-called 'dynamic' ADI to strongly coupled second-order equations and shown that the splitting method requires an order of magnitude less storage and is an order of magnitude faster. The coordinate splitting requires special approach in case of complex domains. The problems connected with applying ADI together with domain composition are treated in [15] where numerical solution is obtained for variety of complex-shaped domains. A new class of time-stepping algorithms is developed in [1] for strongly coupled thermomechanical problems.

To the best of our knowledge, the coordinate splitting methods have not been applied to parabolic equations with higher-order diffusion operators. In the present work we corroborate the technique of splitting with application to the higher-order diffusion equations containing fourth-order diffusion. We demonstrate the performance of the technique on the bifurcation problem for the so-called Swift–Hohenberg equation arising in the study of Rayleigh–Bénard convection.

2. Posing the problem

Consider the fourth-order PDE

$$\frac{\partial u}{\partial t} = -\Delta\left[a_4(x,y,t)\,\Delta u\right] + \nabla\left[a_2(x,y,t)\nabla u\right] - a_0(x,y,t)u - b(x,y,t) + F(u)\,, \tag{2.1}$$

$$\Delta \equiv \frac{\partial^2}{\partial x^2} + \frac{\partial^2}{\partial y^2}\,, \tag{2.2}$$

Eq. (2.1) is a typical generalization of the diffusion equation when a higher-order diffusion is concerned. Its main feature is that the diffusion is represented by the fourth-order derivatives, while depending on the sign of a_2, the second-order derivatives may represent either dissipative or energy pumping mechanism. This effect in $1D$ is well known from the works on KS equation and its generalizations ([9,16,6])

Consider a rectangular region $D : x \in [0, L_x,], y \in [0, L_y]$. The boundary of the region D is denoted by ∂D. Different types of b.c. can be considered from the physical point of view. In order to figure out the correct sets of b.c. we consider the difference $v = u_1 - u_2$, where u_1, u_2 are two solutions satisfying the same b.c. For the new function we have the same equation (2.1) but without the term $b(x,y,t)$. Upon multiplying it by v and integrating over the domain D we get

$$\begin{aligned}\frac{\mathrm{d}}{\mathrm{d}t}\frac{1}{2}\int_D v^2\,\mathrm{d}x\,\mathrm{d}y = &-\oint_{\partial D} v\,\frac{\partial a_4(x,y,t)\,\Delta v}{\partial n}\,\mathrm{d}l - \oint_{\partial D} a_4(x,y,t)\,\Delta v\,\frac{\partial v}{\partial n}\,\mathrm{d}l\\ &-\oint_{\partial D} a_2(x,y,t)v\,\frac{\partial v}{\partial n}\,\mathrm{d}l - \int_D a_0(x,y,t)(\Delta v)^2\,\mathrm{d}x\,\mathrm{d}y\\ &-\int_D a_2(x,y,t)(\nabla v)^2\,\mathrm{d}x\,\mathrm{d}y - \int_D a_0(x,y,t)v^2\,\mathrm{d}x\,\mathrm{d}y\end{aligned} \tag{2.3}$$

The correct set of b.c. is the one which secures that the evolution of the 'energy' $\int v^2$ depends only on its production or dissipation in the bulk, but not on the surface. Investigating the correctness and pertinence to physical problems of the case when production or dissipation are possible at the boundaries, goes beyond the scope of the present work. Whatever the b.c. are, for v they become homogeneous due to definition. Then we are free to select any set of conditions that renders equal to zero the surface integrals in (2.3). These b.c. are

$$v = \frac{\partial v}{\partial n} = 0\,, \qquad v = \Delta v = 0\,, \qquad \frac{\partial v}{\partial n} = \frac{\partial \Delta v}{\partial n} = 0\,, \qquad \Delta v = \frac{\partial \Delta v}{\partial n} = 0 \quad \text{for } (x,y) \in \partial D\,. \tag{2.4}$$

where n stands for the outer normal direction to the boundary ∂D.

The first two sets of admissible b.c. we call 'generalized Dirichlet conditions' of first $(2.4)_1$ and second $(2.4)_2$ kind, respectively. The rest of b.c. involve only derivatives at the boundary, hence the coinage—'generalized Neumann conditions'. Note that the second of the Neumann conditions $(2.4)_4$ can be used only if the original equation does not contain second-order operators , i.e., when $a_2 \equiv 0$. Hence, we consider only the Neumann conditions of first kind $(2.4)_3$. Returning to the original function u one can use the same form of the b.c., simply replacing the zeros by certain given functions of the independent variable at the boundary.

3. The splitting

It is convenient to introduce the following formal notations for the different operators

$$\begin{aligned} L_1 &\equiv -\frac{\partial^2}{\partial x^2}\, a_4(x,y,t)\, \frac{\partial^2}{\partial x^2} - \frac{1}{2}\, a_0(x,y,t) + \left.\frac{\partial F}{\partial u}\right|^n\,, \qquad L_{xx} \equiv \frac{\partial}{\partial x}\, a_2(x,y,t)\, \frac{\partial}{\partial x}\,, \\ L_2 &\equiv -\frac{\partial^2}{\partial y^2}\, a_4(x,y,t)\, \frac{\partial^2}{\partial y^2} - \frac{1}{2}\, a_0(x,y,t) + \left.\frac{\partial F}{\partial u}\right|^n\,, \qquad L_{yy} \equiv \frac{\partial}{\partial y}\, a_2(x,y,t)\, \frac{\partial}{\partial y}\,, \\ L_{12} &\equiv -\frac{\partial^2}{\partial x^2}\, a_4(x,y,t)\, \frac{\partial^2}{\partial y^2} - \frac{\partial^2}{\partial y^2}\, a_4(x,y,t)\, \frac{\partial^2}{\partial x^2}\,. \end{aligned} \tag{3.1}$$

First, we show the desired form of the first-order in time implicit scheme for (2.1) in full time steps. According to the role of the different terms they are taken either on the 'new' or on the 'old' time stage. For the boundary conditions considered here, the mixed fourth derivative is an oblique operator and does not affect the stability, but if taken on the 'new' time stage it spoils the structures of the matrices to be inverted at the semi-half time steps when splitting is effected. For this reason it is left on the 'old' time stage. Then the implicit scheme reads

$$\frac{u^{n+1} - u^n}{\tau} = (L_1 + L_2 + L_{xx} + L_{yy})u^{n+1} + 2L_{12}u^n - b(x,y,t^{n+1}) \tag{3.2}$$

whose equivalent form is as follows

$$\left[E - \tau(L_1 + L_2 + L_{xx} + L_{yy})\right] u^{n+1} = u^n + \tau\left\{L_{12}u^n - b(x,y,t^{n+1}) + \left[F(u^n) - \left.\frac{\partial F}{\partial u}\right|^n u^n\right]\right\}\,. \tag{3.3}$$

where E is the unit operator. We call in what follows scheme (3.2) 'scheme I' or 'implicit scheme'.

It is not clear a priori which is the adequate stage ('old' or 'new') for the second spatial derivatives. When $a_2 > 0$, the additional diffusion due to the second derivatives can be treated in precisely the same manner as the one due to the fourth derivatives. Complications arise when $a_2 < 0$, since depending on the size of region D (and hence on the steepness of the solution itself), the linear spatial operator may cease to be negative definite. A simple consequence of this fact is the occurrence of a linear bifurcation of the stationary problem. We face this complication with a modified scheme, namely

$$\frac{u^{n+1} - u^n}{\tau} = (L_1 + L_2)u^{n+1} + (L_{12} + L_{xx} + L_{yy})u^n - b(x,y,t^{n+1}) + \left.\frac{\partial F}{\partial u}\right|^n (u^{n+1} - u^n) + F(u^n), \tag{3.4}$$

or equivalently,

$$\begin{aligned} &[E - \tau(L_1 + L_2)]u^{n+1} = u^n + \tau f^{n+1} + (L_{xx} + L_{yy})u^n, \\ &f^{n+1} \equiv 2L_{12}u^n - b(x,y,t^{n+1}) + \left[F(u^n) - \left.\frac{\partial F}{\partial u}\right|^n u^n\right]\,. \end{aligned} \tag{3.5}$$

Hereafter we call (3.4) or (3.5) 'scheme II' or 'semi-implicit' scheme.

Each of the systems (3.3), (3.5) results in a three-dimensional matrix of 'stereo-five diagonal' structure. The inversion of this kind of matrix is an expensive procedure even though it is sparse. The 3D case is specially expensive. The physically most acceptable way to reduce the complexity of the problem is to use coordinate splitting which was originated for the parabolic equations in Fifties [3] (see also [19] for review of the parallel soviet works).

The first thing one can do here is to generalize the so-called Alternating Directions Implicit scheme (ADI) [3,13]. However, the ADI scheme is at its stability margin and the inclusion of nonlinear terms could bring into play considerable limitations on the time increment. That is why we prefer the 'scheme of stabilizing correction' or also called *second Douglas scheme* (see [19]) which is more robust for nonlinear problems than ADI. Another advantage of the stabilizing correction is that it is stable in 3D while ADI is not even for linear problems. The only disadvantage is that the second Douglas scheme is first order in time. In terms of the notations of the present work, we have for scheme I the following

$$\begin{aligned} &\frac{\tilde{u}-u^n}{\tau} = (L_1 + L_{xx})\tilde{u} + (L_2 + L_{yy} + L_{yy})u^n + f^{n+1}, \\ &\frac{u^{n+1}-\tilde{u}}{\tau} = (L_2 + L_{yy})(u^{n+1} - u^n) \end{aligned} \tag{3.6}$$

In order to show that the splitting scheme approximates the original implicit scheme we rewrite (3.6) as follows

$$\begin{aligned} &[E - \tau(L_1 + L_{xx})]\tilde{u} = [E + \tau(L_2 + L_{yy})]u^n + f^{n+1}, \\ &[E - \tau(L_2 + L_{yy})]u^{n+1} = \tilde{u} - \tau(L_2 + L_{yy})u^n \end{aligned} \tag{3.7}$$

Now we are prepared to exclude the intermediate variable $\tilde{u}$. This is done after applying the operator $[E - \tau(L_1 + L_{xx})]$ to the second of equations (3.7) and adding the result to the first one, namely

$$[E + \tau(L_1 + L_{xx})][E - \tau(L_2 + L_{yy})]u^{n+1} = \tag{3.8}$$

$$[E - \tau(L_2 + L_{yy})]u^n - \tau[E - \tau(L_1 + L_{xx})](L_2 + L_{yy})u^n + f^{n+1}, \tag{3.9}$$

or else,

$$[E - \tau^2(L_1 + L_{xx})(L_2 + L_{yy})]\frac{u^{n+1}-u^n}{\tau} = (L_1 + L_2 + L_{xx} + L_{yy})u^{n+1} + f^{n+1}. \tag{3.10}$$

The latter is in fact (3.2) save the operator

$$B \equiv E + \tau^2(L_1 + L_{xx})(L_2 + L_{yy}) = E + \mathrm{O}(\tau^2), \tag{3.11}$$

acting upon the time difference $u^{n+1} - u^n/\tau$. One sees that the time splitting scheme approximates the original scheme I within the order $\mathrm{O}(\tau^2)$, which is better than the order of approximation of the latter. Thus, employing a splitting does not degrade the temporal approximation of the scheme. In other words, the splitting scheme coincides with the original scheme within the order of approximation of the latter.

When the norm of the operator B is greater than unity the splitting scheme is even more stable than the original one. However, it may not always be the case when $a_2 < 0$. To treat the last case, we formulate the splitting for scheme II in a similar fashion

$$[E - \tau L_1]\tilde{u} = [E + \tau L_2]u^n + \tau(L_{yy} + L_{xx})u^n + f^{n+1}, \tag{3.12}$$

$$[E - \tau L_2]u^{n+1} = \tilde{u} - \tau L_2 u^n \tag{3.13}$$

Upon excluding the auxiliary variable we arrive at

$$[E + \tau^2 L_1 L_2]\frac{u^{n+1}-u^n}{\tau} = (L_1 + L_2)u^{n+1} + (L_{xx} + L_{yy})u^n + f^{n+1}. \tag{3.14}$$

and now the operator

$$B \equiv E + \tau^2 L_1 L_2 = E + \mathrm{O}(\tau^2), \tag{3.15}$$

has a norm greater than unity. The two different schemes proposed here perform on generally equal level for strictly diffusive problems ($a_2 > 0$), but differ qualitatively when bifurcation problems ($a_2 < 0$), are treated.

4. Spatial discretization

Consider a staggered mesh in both spatial directions, namely

$$x_i = -\frac{h_x}{2} + i\,h_x, \qquad h_x \equiv \frac{L_x}{M-2}, \qquad y_i = -\frac{h_y}{2} + j\,h_y, \qquad h_y \equiv \frac{L_y}{N-2}, \tag{4.1}$$

where M, N are the number of points in x, y directions, respectively. Let $\Phi_{i,j}$ be an arbitrary set function defined on the above described mesh. We confine ourselves to the case of constant coefficients. Then the simplest symmetric difference approximations of the differential operators read

$$\begin{aligned}
\Lambda_1 \Phi i, j &= -\frac{\Phi_{i+2,j} - 4\Phi_{i+1,j} + 6\Phi i, j - 4\Phi_{i-1,j} + \Phi_{i-2,j}}{h_x^4} \\
\Lambda_2 \Phi i, j &= -\frac{\Phi_{i,j+2} - 4\Phi_{i,j+1} + 6\Phi i, j - 4\Phi_{i,j-1} + \Phi_{i,j-2}}{h_y^4} \\
\Lambda_{12} \Phi i, j &= -\frac{1}{h_x^2 h_y^2}[\Phi_{i+1,j+1} - 2\Phi_{i+1,j} + \Phi_{i+1,j-1} - 2(\Phi_{i,j+1} - 2\Phi_{i,j} + \Phi_{i,j-1}) \\
&\quad + \Phi_{i+1,j+1} - 2\Phi_{i+1,j} + \Phi_{i+1,j-1}] \\
\Lambda_{xx} \Phi_{i,j} &= \frac{\Phi_{i+1,j} - 2\Phi_{i,j} + \Phi_{i-1,j}}{h_x^2}, \qquad \Lambda_{yy} \Phi_{i,j} = \frac{\Phi_{i,j+1} - 2\Phi_{i,j} + \Phi_{i,j-1}}{h_x^2}
\end{aligned} \tag{4.2}$$

Here the notation Λ stands for the discrete approximation of the respective operator L.

On the staggered mesh, any kind of b.c. are easily approximated with second-order approximation, namely

$$\begin{aligned}
&u_{1,j} + u_{2,j} \approx 2u\,|_{x=0}, \qquad u_{3,j} - u_{2,j} - u_{1,j} + u_{0,j} \approx 2h_x^2 \left.\frac{\partial^2 u}{\partial x^2}\right|_{x=0}, \\
&u_{2,j} - u_{1,j} \approx h_x \left.\frac{\partial u}{\partial x}\right|_{x=0}, \qquad u_{M+1,j} - 3u_{M,j} + 3u_{M-1,j} + u_{M-2,j} \approx 6h_x^3 \left.\frac{\partial^3 u}{\partial x^3}\right|_{x=L_x}, \\
&u_{M-1,j} + u_{M,j} \approx 2u\,|_{x=L_x}, \qquad u_{M+1,j} - u_{M,j} - u_{M-1,j} + u_{M-2,j} \approx 2h_x^2 \left.\frac{\partial^2 u}{\partial x^2}\right|_{x=L_x}, \\
&u_{M,j} - u_{M-1,j} \approx h_x \left.\frac{\partial u}{\partial x}\right|_{x=L_x}, \qquad u_{3j} - 3u_{2j} + 3u_{1j} + u_{0j} \approx 6h_x^3 \left.\frac{\partial^3 u}{\partial x^3}\right|_{x=0},
\end{aligned} \tag{4.3}$$

for $j = 3, \ldots, N-2$ and

$$
\begin{aligned}
&u_{i,1} + u_{i,2} \approx 2u\,|_{y=0}\,, \qquad u_{i,3} - u_{i,2} - u_{i,1} + u_{i,0} \approx 2h_y^2 \left.\frac{\partial^2 u}{\partial y^2}\right|_{y=0}\,,\\
&u_{i,2} - u_{i,1} \approx h_y \left.\frac{\partial u}{\partial y}\right|_{y=0}\,, \qquad u_{i,3} - 3u_{i,2} + 3u_{i,1} + u_{i,0} \approx 6h_y^3 \left.\frac{\partial^3 u}{\partial y^3}\right|_{y=0}\,,\\
&u_{i,N-1} + u_{i,N} \approx 2u|_{x=L_y}\,, \qquad u_{i,N+1} - u_{i,N} - u_{i,N-1} + u_{i,N-2} \approx 2h_y^2 \left.\frac{\partial^2 u}{\partial y^2}\right|_{y=L_y}\,,\\
&u_{i,N} - u_{i,N-1} \approx h_y \left.\frac{\partial u}{\partial y}\right|_{y=L_y}\,, \qquad u_{i,N+1} - 3u_{i,N} + 3u_{i,N-1} + u_{i,N-2} \approx 6h_y^3 \left.\frac{\partial^3 u}{\partial y^3}\right|_{y=L_y}\,,
\end{aligned}
\tag{4.4}
$$

for $i = 3, \ldots, N-2$.

One sees that the values of the sought function in these mesh points are also never used in the scheme. In this sense, the staggered mesh is consistent. One can extrapolate the values of the function in these points after the calculations are completed for the given time step.

5. Tests and verifications

The first mandatory test for a splitting scheme is to show that it can successfully serve as an iterative procedure to the stationary solution. In order to verify this property for our scheme we consider only the linear part of the problem

$$
\frac{\partial u}{\partial t} = -\Delta\Delta u - 2\Delta u - u - 1, \tag{5.1}
$$

in the unit square. For the sake of completeness of the test we solve the problem (5.1) with the two kinds of Dirichlet b.c. For the sake of simplicity, the initial condition is taken to be equal to zero.

It is clear that after sufficient number of time steps, the solution of (5.1) converges to the stationary pattern compatible with the operator in the right hand side and with the b.c. (the solution of the steady problem). It is important to show that the stationary solution that is obtained after the convergence does not depend on the magnitude of the time increment. The term containing τ in the 'full-step' scheme (3.10) supposedly vanishes when the number of time-steps increases and $u^{n+1} \longrightarrow u^n$. Our numerical experiments with the test case did indeed verify that the implementation of the scheme does possess the said property. To this end we used three different measures of convergence

$$
\begin{aligned}
&L_u \equiv \max \left| \frac{u_{ij}^{n+1} - u_{ij}^n}{\tau\, u_{ij}^{n+1}} \right|, \qquad L_1 \equiv \frac{\sum_{ij} \left| u_{ij}^{n+1} - u_{ij}^n \right|}{\tau \sum_{ij} \left| u_{ij}^{n+1} \right|}\\
&L_2 \equiv \sqrt{\frac{1}{\tau MN \max \left| u_{ij}^{n+1} \right|} \sum_{ij} \left(u_{ij}^{n+1} - u_{ij}^n \right)^2},
\end{aligned}
\tag{5.2}
$$

called uniform, L_1 and L_2, respectively. Our experience shows that the first norm was too restrictive and required a large number of time steps in order to reach convergence. The other two norms perform on the same level, but the L_1 is significantly less expensive in the sense of number of operations involved in the calculation. The experiments clearly indicate that the steady solution does not depend on the magnitude of the time increment which is a verification of the property under consideration.

The next important property of the scheme is the spatial approximation. In order to assess the latter we perform the calculations with four different meshes decreasing each time the spacing twice. Fig. 1(a) shows the dependence of solution on the mesh size for the case of Dirichlet boundary conditions of first kind. The agreement between the different curves is very good. Even for the extremely rough mesh with 16×16 points the deviation is less than 4%. The case of Dirichlet b.c. of second kind is more sensitive

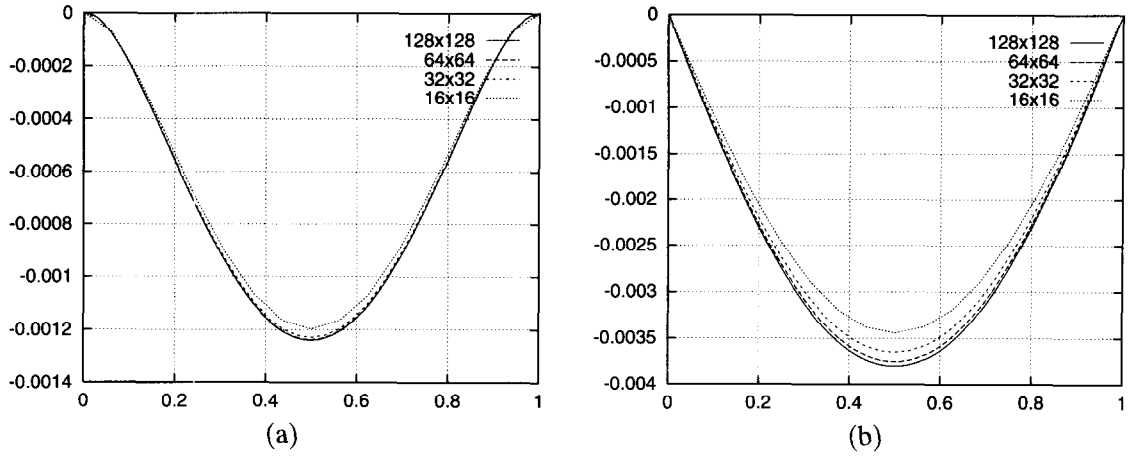

Fig. 1. Comparison of results with different mesh sizes for Dirichlet b.c. in a cross section: (a) first kind; (b) second kind.

to the values of mesh parameters due to the greater flexibility allowed by those b.c. Yet the deviation for the rougher mesh is still less than 10% (Fig. 1(b)).

The results of the present Section suffice to claim that the difference scheme is constructed correctly and represent adequately the differential operators.

6. Treating bifurcation problems. Application to the S–H equation

Regardless of the complicated structure of the differential operator, the example considered in the previous Section is a simple one, in the sense that because of the small size of the domain, the stationary problem possesses a unique solution for each of the considered sets of b.c. and it is monotone approached by the iterative procedure. As earlier mentioned, the improper sign of the second derivatives can bring about a linear bifurcation of the problem. The bifurcation and branching of non-trivial solutions is the most interesting trait of the Generalized Parabolic Equation under consideration. Consider the following version of (2.1)

$$\tau_0 \frac{\partial u}{\partial t} = -D(\Delta + \kappa^2)^2 + F(u) \equiv -\Delta\Delta u - 2\kappa^2 \Delta u - \kappa^4 + F(u)\,. \tag{6.1}$$

In the case of cubic nonlinearity,

$$F(u) \equiv \varepsilon u - g u^3\,, \tag{6.2}$$

the eq.(6.1) is the Swift–Hohenberg equation (S–H, for brevity) derived for the Rayleigh–Bénard convection to account for the formation of convective rolls in high Prandtl number fluid layers [17]. It turned out to possess greater applicability for describing pattern formation in two dimensions [11]. Apparently, it looks like a typical generalization of the diffusion equation when a higher-order diffusion is concerned, but it cannot be called 'diffusion equation' in the strict sense of the word, due to the improper sign of the second derivatives. The main feature of (6.1) is that the damping of inhomogeneous perturbations occurs via the fourth-order spatial derivatives, while these perturbations are enhanced by the second-order spatial derivatives the latter having an anti-diffusive behavior. A similar effect in 1D is well known from the study of the KS equation ([9,16,6]). Here, the difference is that the SH admits Lyapunov function

$$\Psi = \int_D \left[-\frac{\varepsilon}{2} u^2 + \frac{g}{4} u^4 + \frac{D}{2} \left((\Delta + \kappa^2) u \right)^2 \right] \mathrm{d}x\,\mathrm{d}y, \qquad \frac{\partial \Psi}{\partial t} = -\tau_0 \int_D \left(\frac{\partial u}{\partial t} \right)^2 \mathrm{d}x\,\mathrm{d}y < 0\,. \tag{6.3}$$

Note that S–H equation admits also a potential coinciding in shape with the Lyapunov function (6.3) (see [11]).

The existence of Lyapunov function rules out possible temporal complex behavior (turbulent or chaotic) in the long times and only allows formation of steady convective patterns as a bifurcation from a (generally, motionless) reference state. These steady patterns can be quite complicated in shape, e.g., spatially chaotic. The convective patterns arise beyond the threshold for bifurcation and occur on account of the interplay between the complicated linear operator and the nonlinearity. From the perspective of GDE it is clear—bifurcation could only take place for sufficiently large domains whose size is commensurate with the length scales of the patterns.

Many aspects of this equation have been studied both analytically and numerically and found to agree with experimental observations. However, in many cases, the bifurcation parameter is not constant and may be spatially nonuniform as in the case of thermal convection in the presence of an horizontal temperature gradient [18]. In this case ε depends on the spatial coordinate x, and no analytical treatment is available in general. Thus one has to rely on the numerical analysis of the dynamics, as we shall illustrate here.

Consider the rectangle $x \in [0, L_x]$, $y \in [0, L_y]$. Different types of b.c. can be considered at its boundary. Except for the periodic conditions, the rest can be separated mainly into two classes: generalizations of the Dirichlet or Neumann conditions. These have already been discussed and explicitly written when the correct posing of the problem was discussed. In the rectangular domain, the Dirichlet b.c. of the first and second kind read

$$u = \frac{\partial u}{\partial x} = 0 \quad \text{for } x = 0,\ L_x; \qquad u = \frac{\partial u}{\partial y} = 0 \quad \text{for } y = 0,\ L_y, \tag{6.4}$$

$$u = \frac{\partial^2 u}{\partial x^2} = 0 \quad \text{for } x = 0,\ L_x; \qquad u = \frac{\partial^2 u}{\partial y^2} = 0 \quad \text{for } y = 0,\ L_y, \tag{6.5}$$

Respectively, the Neumann condition is

$$\frac{\partial u}{\partial x} = \frac{\partial^2 u}{\partial x^2} = 0 \quad \text{for } x = 0,\ L_x, \qquad \frac{\partial u}{\partial y} = \frac{\partial^2 u}{\partial y^2} = 0 \quad \text{for } y = 0,\ L_y, \tag{6.6}$$

Combinations of Dirichlet and Neumann conditions can be used at the different boundaries, but for simplicity we do not consider the mixed types of conditions. It is clear that if the same scheme and algorithm perform properly for the 'pure' cases (including the Neumann one), then they will do the same for the mixed cases, since any admissible (in the sense of (2.3)) mixture of conditions yields to a well posed boundary value problem.

Next, it is important to validate the performance of the scheme for bifurcation problems. The coefficients τ_0, g and D reflect the physical properties of the fluid layer. We set for definiteness τ_0, $\kappa = 3.1172 \approx \pi$, $g = 12.9$, $D = 0.015$ which corresponds to the typical pattern excitation in Rayleigh–Bénard convection ([18,2,12]). Upon employing these values the amplitude equation obtained from S–H equation describing the time evolution of a single-mode structure coincides with the amplitude equation derived directly from the Navier–Stokes equations [14]. Note that this is not the eigen-value of the present problem, because with the non-constant bifurcation parameter, the linear stability analysis could not be carried out analytically.

We consider the case when the bifurcation parameter is linear function of the coordinate x (for definiteness $\varepsilon = -0.1 + 0.01x$), which has important implications for the convective patterns [18]. We begin with the case of Dirichlet b.c of first kind (6.4). We select a region of size $H_x = 20$, $H_y = 20$ which we call in what follows 20×20 box. The calculations start from random initial condition and the iterations are conducted until convergence. The stationary solutions we obtained with different time increments (changing the time increment up to 20 times) differ less than 0.02% which is a practical demonstration of the fact that the scheme possess so-called 'full approximation' [19]. It is clear that the larger the box is, the larger the number of nontrivial solutions is. Fig. 2 illustrates the shape of the branching solution for a relatively small box and for the above specified ε.

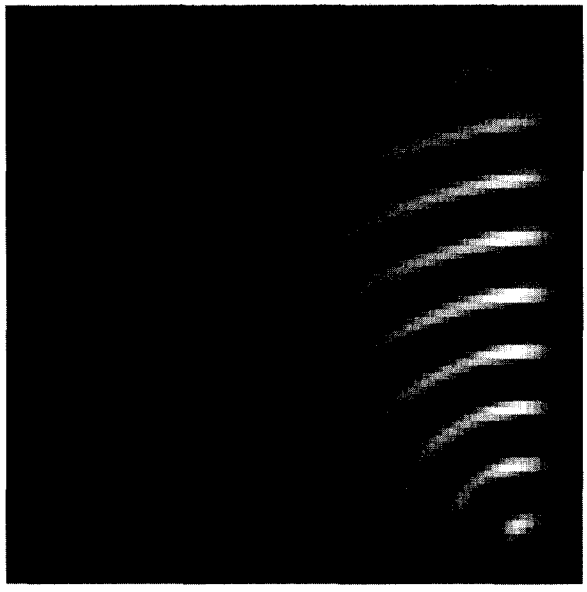

Fig. 2. The convective pattern for the 20 × 20 box and $\varepsilon = -0.1 + 0.01x$.

Note that for this system of relatively small size the two schemes I and II performed with roughly the same efficiency. In Fig. 3 is shown the convergence in terms of L_1 norm to the stationary solution for a box of dimensions 20 × 20. The solid line presents the performance of the fully implicit scheme. It is seen that for the same value of the time increment, the implicit scheme I converges more rapidly than the semi-explicit scheme II. The crucial difference is, however, that the semi-explicit scheme allows time increments that are up to 20 times larger than those admissible by the implicit one and that is what makes it the better choice for treating the bifurcation problem. We mention here that the regions of non-monotone behavior of the L_1 norm correspond to swift rearrangements of the pattern. These are exactly the time intervals where the fully implicit scheme diverges for large time increments. As earlier explained, the divergence is a consequence of the intricate interplay between the different components of the operator making its inversion an ill-posed problem.

One should not be deceived here by the apparent slowing down of the slope of L_1 norm as a function of time with increasing the time increment for the semi–implicit scheme. In fact the amount of computational time spent decreases when the time increment increases to approximately $\tau = 1$. For larger τ the computational time increases again. Hence, the conclusion is that $\tau = 1$ is the optimal time increment for the box under consideration. We note that the optimal value of τ depends very much on the size of the region, since it is defined by the ratio of the eigen-values of the stationary problem.

Another example is furnished for the same bifurcation parameter by the pattern in the still smaller box 20 × 10, shown in Fig. 4. We use it also to demonstrate that the bifurcation property does not depend on the magnitude of spacings! Although we have already shown the spatial convergence of the scheme when treating the linear test problem, the test for the branching solution is not a trivial one, insofar as more than one non-trivial solution may exist. Then depending on the grid resolution, the algorithm may converge to one or another. In this case we do not start from the random initial condition, because on different meshes it is different. Rather we start from an initial distribution which is everywhere equal to zero, save a single point in which the functional value is set equal to one. We refer to this initial condition as 'numerical delta function'. The results of different calculations for the 20 × 10 box are presented in the sequence of Fig. 4. It is seen that the solution remains the same within the adopted order of approximation. The spatial convergence of the solution can be appreciated better from the cross-section for $y = 5$ presented in Fig. 5. One sees that only the roughest-mesh results differ from the

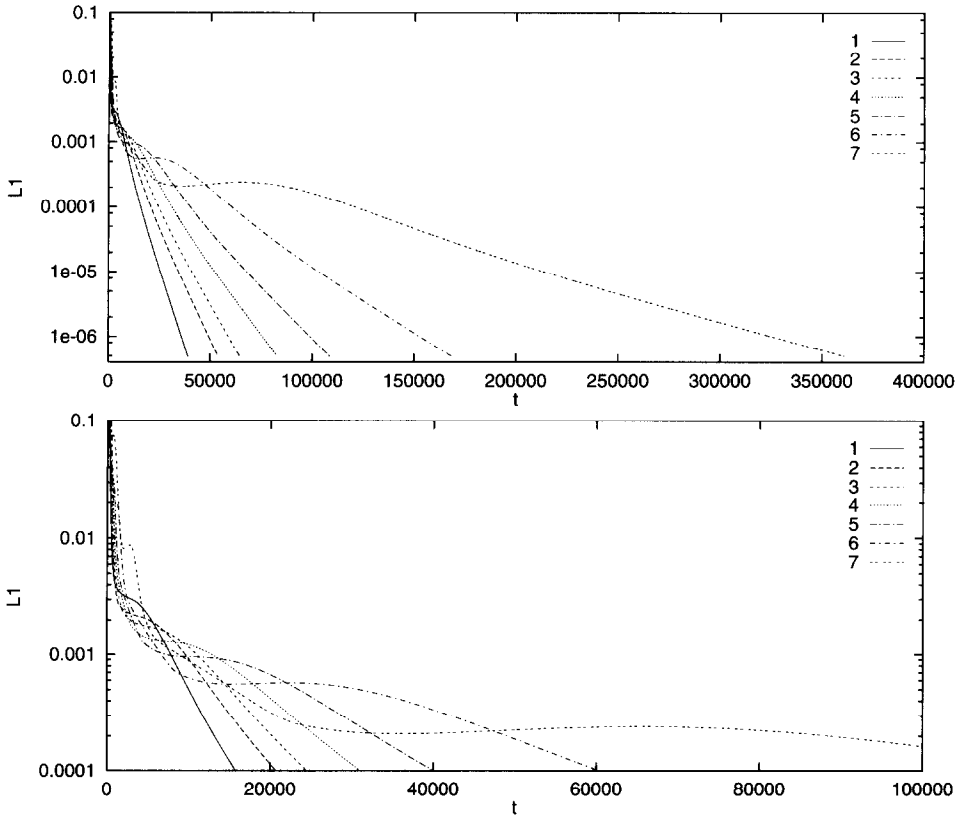

Fig. 3. Convergence in terms of L_1 norm for the 20×20 box and $\varepsilon = -0.1 + 0.01x$. The lower graph is a zoom on the upper: (1) – $\tau = 0.14$ (scheme I); (2) – $\tau = 0.14$; (3) – $\tau = 0.24$; (4) – $\tau = 0.40$; (5) – $\tau = 0.60$; (6) – $\tau = 1.0$; (7) – $\tau = 2.0$

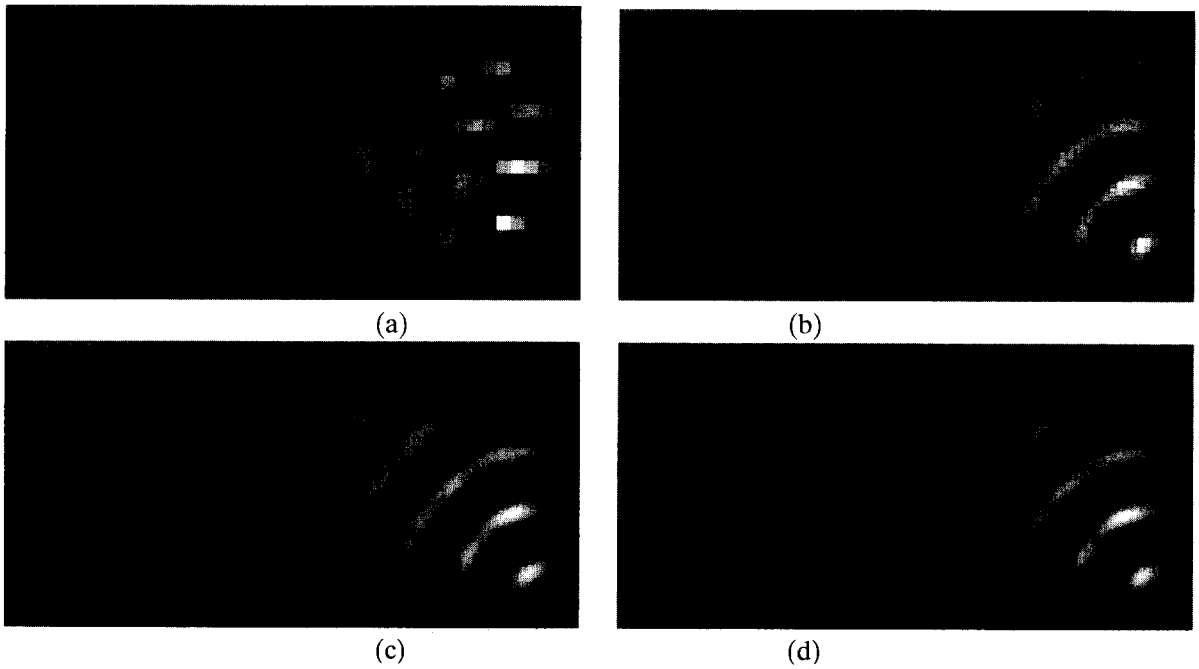

Fig. 4. The convective pattern for the 20×10 box obtained with different resolutions: (a) 40×20; (b) 80×40; (c) 160×80; (d) 320×160.

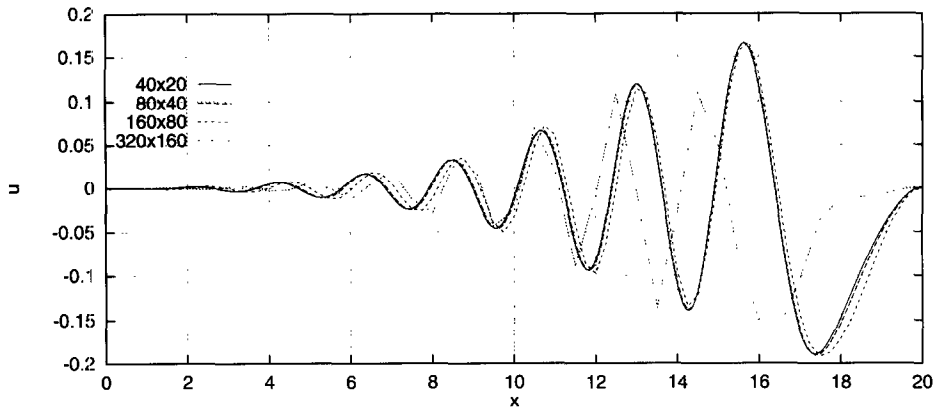

Fig. 5. A cross-section $y = 5$ of the solution from Fig. 4.

rest and still only by a phase error. The conclusion is that the scheme presented here is accurate enough for treating bifurcation with Dirichlet b.c.

It is interesting to investigate the behavior of the branching solution for even higher super-criticalities (larger dimensions of the box). On the other hand, there are reasons to believe that there exist solutions in which the rolls align parallel to the shorter side. As already above mentioned, the solution for large boxes is by no means unique. In order to discover a solution of the desired type of alignment, one has to impose initial conditions which belong to the basin of attraction of the sought solution. For this reason we consider now the case of $\varepsilon = 0.01x$ with different transverse dimensions of the box. The initial conditions are simply rolls aligned with the shorter side. These initial conditions do not satisfy the b.c. on the vertical sides, and hence, the test is not trivial. After the convergence is attained, the stationary solution is found. Figs. 6 show the solution. The major conclusion is that the wall mode (the longitudinal profile of a roll) does not depend on the transverse size of the box. Fig. 7 shows the profile of the solution as a function of the longitudinal variable x, for a given value of y. The quantitative agreement between the profile of the wall mode for different boxes is very good. Thus, one sees that alignment of rolls is a property of the solution of the differential system which is accurately represented by our scheme.

Because the Neumann boundary conditions are more severe tests of a numerical scheme, it is important to examine also the performance of the scheme with the b.c. (6.6). The result for the 20×20 box which otherwise has the same parameters as the one of Fig. 2 is shown in Fig. 9. Respectively, Fig. 10 presents the evolution of the L_1 norm for the same case. It is of special importance the fact that we encountered here more rapid convergence than is expected for a Neumann problem. It is well known that if the equation consisted only of the differential operators then the Neumann problem would have been incorrect in the sense that its solution is defined only up to an additive constant. As a rule, this reflects in a somewhat slower convergence for the correct problem. It is instructive to note that we have not discovered significant reduction in the speed of convergence from the Dirichlet benchmark even for the problem with four Neumann b.c., presented in Fig. 9.

Finally, we consider a really difficult case of an extremely large box 50×50. Note that due to the choice $\kappa \approx \pi$, our box of dimensions $50\pi \times 50\pi$ compares to a 156×156-box in terms of the scales of [7]. The Lyapunov function (6.3) secures that eventually one of the steady solutions will be reached. The problem is that for such a large box the steady solutions can be numerous and depending on the initial conditions (random in this experiment) the 'trajectory' wanders a very long time between the different states in the functional space, before converging to one of them (the most stable). Fig. 11 shows the evolution for extremely long times (of order of $2 - 3 \times 10^6$). Respectively, Fig. 12 depicts the evolution of the L_1 norm. The jumps correspond to the time intervals of swift rearrangements of the pattern. After

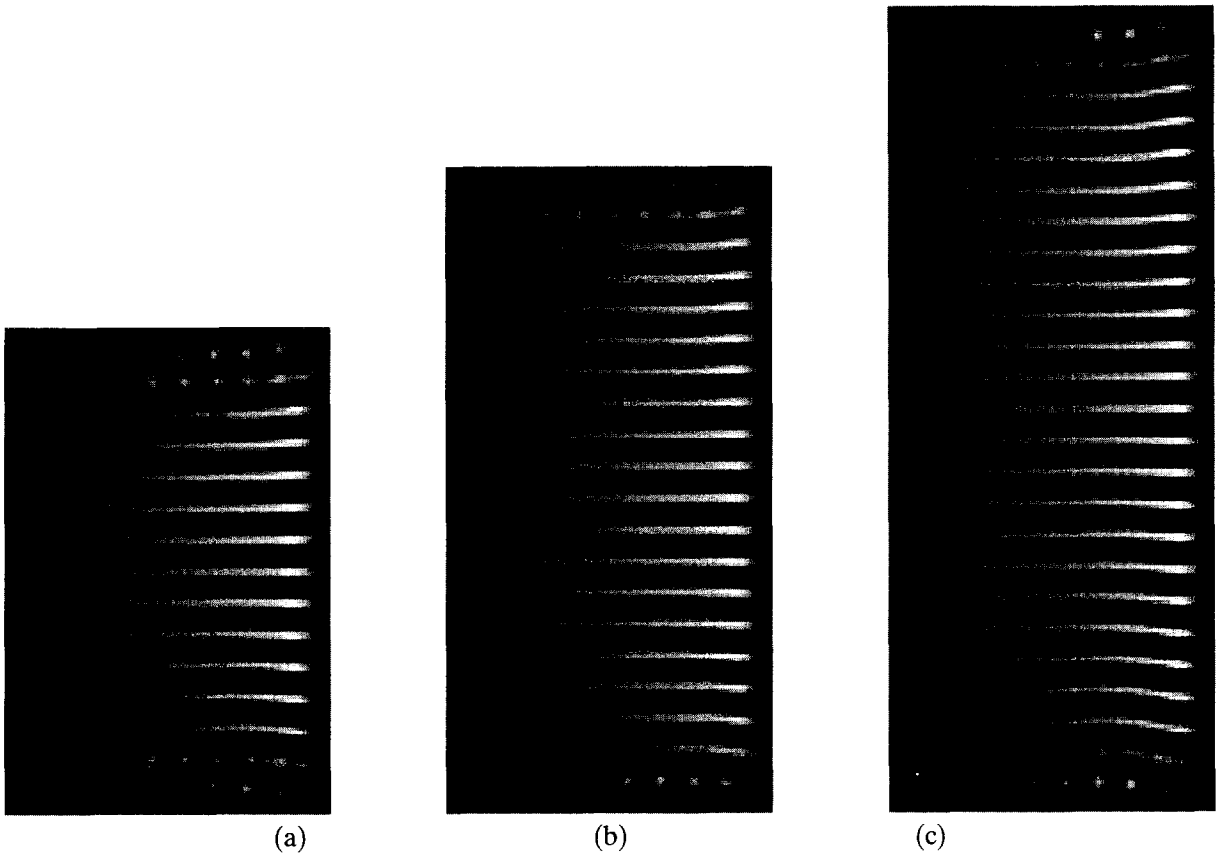

Fig. 6. The alignment of the rolls for $\varepsilon = 0.01x$ and different boxes: (a) 20×30; (b) 20×40; (c) 20×50.

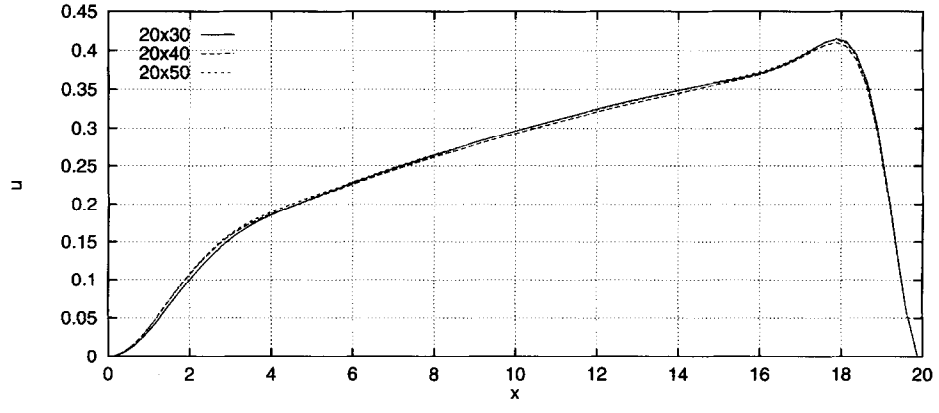

Fig. 7. Comparison of the profiles of the solution for the same y cross-section form Fig. 6.

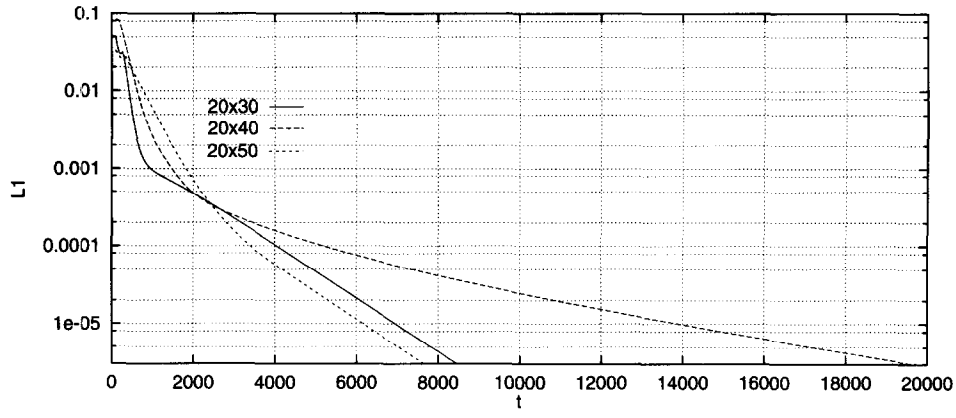

Fig. 8. $L1$ norm for the case from form Fig. 6.

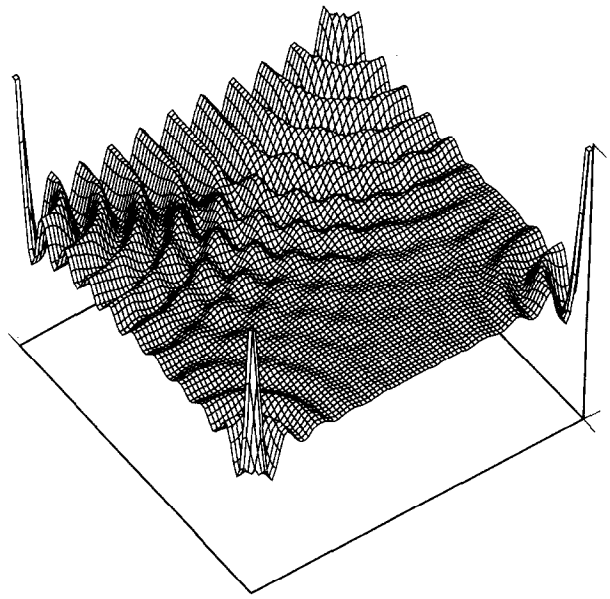

Fig. 9. Solution for Neumann ('soft') b.c. when the bifurcation parameter and the size of system are the same as in Fig. 2.

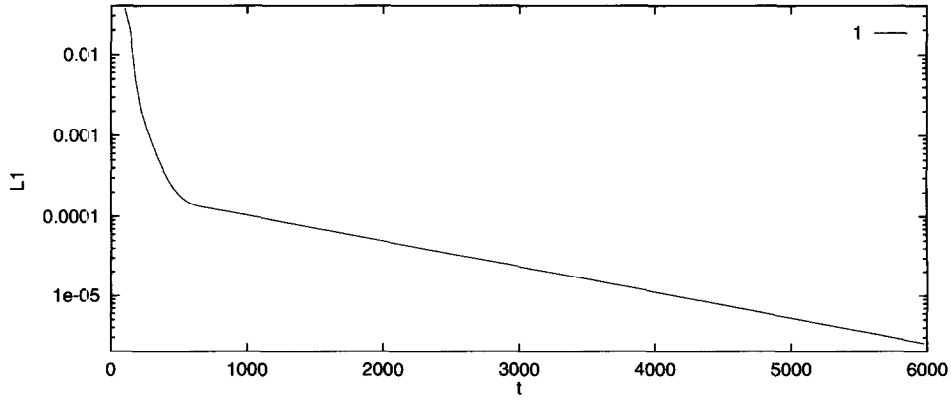

Fig. 10. Evolution of the L_1 norm for the case of Neumann b.c. shown in Fig. 9.

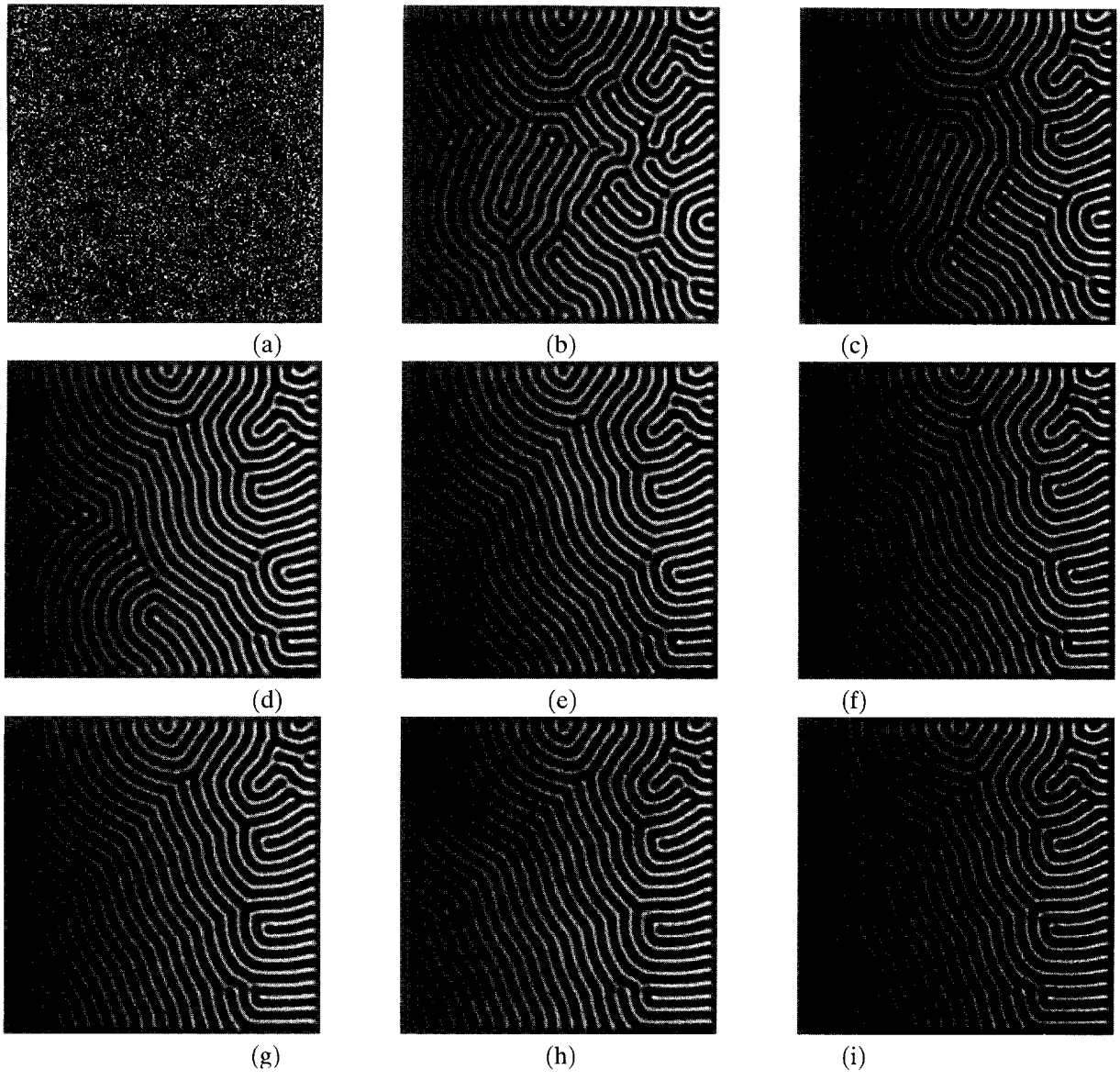

Fig. 11. The temporal evolution of a very large system (50 × 50 box) from a random initial condition: (a) $t = 0$; (b) $t = 4000$; (c) $t = 60000$; (d) $t = 200000$; (e) $t = 300000$; (f) $t = 320000$; (g) $t = 10^6$; (h) $t = 2 \times 10^6$; (i) $t = 2.8 \times 10^6$.

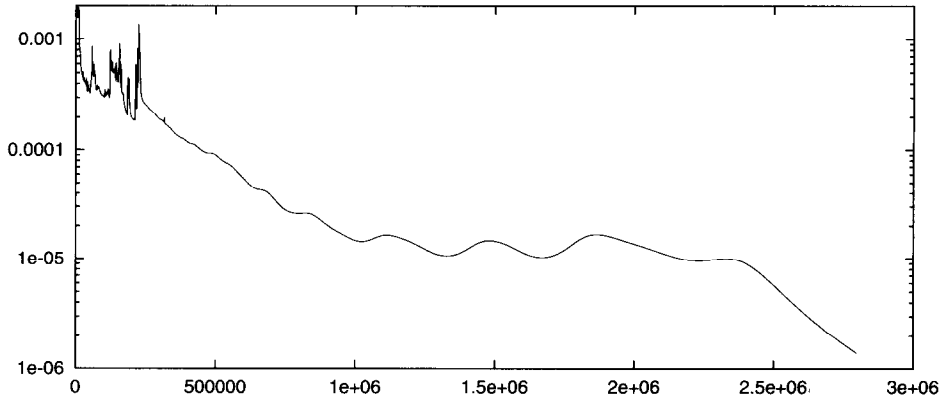

Fig. 12. Evolution of the L_1 norm for the case shown in Fig. 11.

a number of such rearrangements, the evolution becomes slower and reaching the relevant steady state requires too much computational time.

The series of patterns in Fig. 11 shows the gradual disappearance of defects during the evolution. One can also see that the density of defects of the stationary pattern increases from the left to the right side of the image, due to the higher forcing to which the system is submitted on this side (the ramp).

7. Concluding remarks

In the present paper a coordinate-splitting difference scheme and algorithm are developed for solving initial-boundary value problems for generalized parabolic equations containing higher-order diffusion. The temporal and spatial approximations of the scheme are checked by means of different grid sizes. The scheme is of 'full' approximation (coinage introduced by N.N. Yanenko) in the sense that the solution of the steady problem does not depend on the magnitude of time increment.

The scheme has been applied also to non-linear bifurcation problems when the second derivatives enter with the improper sign and play the role of energy pumping in S–H equation, rather than diffusion. Then the balance between the fourth-order operator on the one hand and second-order operator and nonlinearity—on the other, yields bifurcation and the accompanying occurrence of a nontrivial solution to the homogeneous boundary value problem. The scheme appears to perform very well in predicting shapes of the branched solutions. Moreover, it is instrumental in the precise estimation of the instability threshold in the case of spatially nonuniform bifurcation parameters. An extensive set of numerical experiments shows that the said threshold is not very sensitive to the mesh parameters (spacings, time increment).

After thorough investigation of medium size domains, where the branching solutions are reasonably good attractors, the numerical tool developed here is applied to systems of very large size where the convergence to a steady state requires extremely long physical times. The efficiency of the splitting splendidly shows up making possible computations on a small-sized workstation SONY NWS–3410. The times reached and sizes of the systems exceeded several times the calculations reported in the literature by teams using supercomputers for solving similar problems.

Acknowledgments

This work was sponsored in part by CEE Grant CI1*–CTG2–006 and by DGICYT (Spain) Grant PB90–264. A NATO Senior Fellowship is gratefully acknowledged by CIC. JP acknowledges a fellowship from the National Council for the Research and Development–CNPq (Brazil) and support from Promon Engenharia (Brazil).

References

[1] F. Armero and J.C. Simo, A new unconditionally stable fractional step method for non-linear coupled thermo-mechanical problems, Int. J. Numer. Methods Engrg. 35 (1992) 737.
[2] S. Chandrasekhar, Hydrodynamic and Hydromagnetic Instability (Dover, New York, 1961).
[3] J. Douglas and H.H. Rachford, On the numerical solution of heat conduction problems in two and three space variables, Trans. Am. Soc. 82 (1956) 421–439.
[4] L. Ekebjaerg and P. Justesen, An explicit scheme for advection–diffusion modelling in two dimensions, Comput. Methods Appl. Mech. Engrg. 88 (1991) 287–297.
[5] A. Frati, Pasquarelli and A. Quarteroni, Spectral approximation toadvection–diffusion problems by fictitious interface method, J. Comput. Phys. 107 (1992) 201–212.
[6] P.L. García-Ybarra, J.L. Castillo and M.G. Velarde, Bénard–Marangoni convection with a deformable interface and poorly conducting boundaries, Phys. Fluids 30 (1987) 2655–2661.
[7] H.S. Greenside and W.M. Coughran, Nonlinear pattern formation near the onset of Rayleigh–Bénard convection, Phys. Rev. A 30 (1984) 398–428.
[8] D.W. Hewett, D.J. Larson and S. Doss, Solution of simultaneous partial differential equations using dynamics adi: Solution of streamlined Darwin field equation, J. Comput. Phys. 101 (1992) 11–24.

[9] Y. Kuramoto and T. Tsuzuki, Persistent propagation of concentration waves in dissipative media far from thermal equilibrium, Progr. Theor. Phys. 55 (1976) 356–369.
[10] F. Mampaey, A stable alternating direction method for simulating multi-dimensional solidification problems, Int. J. Numer. Methods Engrg. 30 (1990) 711–728.
[11] P. Manneville, Dissipative Structures and Turbulence (Academic Press, San Diego, 1990).
[12] C. Normand, Y. Pomeau, and M.G. Velarde, Convective instability. A Physicist's approach, Rev. Mod. Phys. 49 (1977) 581–601.
[13] D.W. Peaceman and H.H. Rachford, Jr., The numerical solution of parabolic and elliptic differential equations, J. Soc. Indust. Appl. Math. 3 (1955) 28–41.
[14] J. Pontes, Pattern formation in spatially ramped Rayleigh–Bébard systems, Ph.D Thesis, Université Libre de Bruxelles, 1994.
[15] M. Rosenfeld and Y. Yassour, The alternating direction multi-zone implicit method, J. Comput. Phys. 110 (1994) 212–220.
[16] G.I. Sivashinsky and D.M. Michelson, On irregular wavy flow of a liquid film down a vertical plane, Progr. Theor. Phys. 63 (1980) 2112–2114.
[17] J. Swift and P.C. Hohenberg, Hydrodynamic fluctuations and the convective instability, Phys. Rev. A 15: (1977) 319–328.
[18] I.C. Walton, On the onset of Rayleigh–Bénard convection in a fluid layer of slowly varying depth, SIAM 67 (1982) 199–216.
[19] N.N. Yanenko, Method of Fractional Steps (Gordon and Breach, NY, 1971).